

SLAC - PUB - 3926
April 1986
(T/E)

AXION BREMSSTRAHLUNG BY AN ELECTRON BEAM*

YUNG SU TSAI

*Stanford Linear Accelerator Center
Stanford University, Stanford, California, 94305*

ABSTRACT

Compact expressions for energy-angle distribution and energy distribution for axion from the electron scattering on an atomic target are derived using the generalized Weizsacker-Williams method. The axion flux from an electron beam dump is estimated. It is also shown that even in a proton beam dump, the mechanism of producing axions is still predominantly due to electrons in the dump.

Submitted to *Physical Review D*

* Work supported by the Department of Energy, contract DE-AC03-76SF00515.

1. INTRODUCTION

A 1.7 MeV object¹ witnessed in the heavy-ion collisions at GSI has stimulated searches for an axion² of this mass range. This calculation deals with the production cross section and flux of axions produced by an electron beam on atomic targets in order to see whether such an object can be produced in the beam dump experiment. Previous calculation by Donnelly *et al.*,³ assumed an axion mass negligible compared with the electron mass. Hence it is inapplicable for the present purpose.

We first calculate the energy-angle distribution, $d\sigma/d\Omega_a dE_a$, of axions produced in the process $e^- + \text{atomic target} \rightarrow e^- + a + \text{anything}$ using the generalized Weizsacker-Williams method.⁴ Atomic screening as well as production from atomic electrons are important in the energy range of interest ($E_a = 1 \sim 100$ GeV). The angle is then integrated out and an expression for $d\sigma/dE_a$ derived. In the beam dump experiment, the energies of the incident electrons as well as e^\pm from the decay of axions are degraded due to emission of bremsstrahlung as these particles go through a thick target. These effects are also considered. Axion production in a proton beam dump is also discussed.

2. GENERALIZED WEIZSACKER-WILLIAMS METHOD

— The energy-angle distribution of axions from the process $e + P_i \rightarrow e + a + P_f$, shown in Fig. 1(a), can be obtained from the Compton-like process $\gamma + e \rightarrow e + a$,

shown in Fig. 1(b), using the following formula:⁴

$$\begin{aligned} & \left[\frac{d\sigma (P_1 + P_i \rightarrow P_2 + k + P_f)}{d(P_1 \cdot k) d(k \cdot P_i)} \right]_{\text{Weizsacker-Williams}} \\ &= \left[\frac{d\sigma (q + P_1 \rightarrow P_2 + k)}{d(P_1 \cdot k)} \right]_{t=t_{min}} \frac{\alpha}{\pi} \frac{\chi}{P_2 \cdot P_i} \end{aligned} \quad (1)$$

where P_1 , P_2 , P_i , P_f and k are four momenta of the incident electron, outgoing electron, initial target particle, final state of the target particle and the axion, respectively. $(\alpha/\pi)\chi$ is the equivalent radiator thickness^{4,5} for the Weizsacker-Williams photon flux and is related to the W_1 and W_2 functions of the target particle in the electron scattering. The target form factors required depend upon the value of minimum momentum transfer t_{min} which is given by

$$t_{min} = \left[\frac{U}{2E_1(1-x)} \right]^2, \quad (2)$$

where

$$U = m_e^2 \ell x + m_e^2 x + \frac{m_a^2 (1-x)}{x},$$

$$x = \frac{E_a}{E_1} \quad \text{and} \quad \ell = \frac{E_1^2 \theta_a^2}{m_e^2}.$$

For $E_1 = 10$ GeV, $\theta_a = 0$, $x = 1/2$ and $m_a = 1.7$ MeV, we have $t_{min}^{1/2} = 3 \times 10^{-4}$ MeV. Since the atomic radius is given by $a = 111 Z^{-1/3}/m_e$, we have $a t_{min}^{1/2} \ll 1$, thus the atomic form factors are needed to calculate χ in our problem. χ can be written as

$$\chi = \chi_{elas} + \chi_{inelas}, \quad (3)$$

where χ_{elas} and χ_{inelas} are calculated using the elastic and inelastic form factors of the atom, respectively. Using some simple atomic form factors, we can^{4,5} show

that:

$$\chi_{elas} = Z^2 \left[\ln \frac{a^2 m_e^2 (1 + \ell)^2}{a^2 t_{min} + 1} - 1 \right] ,$$

and

$$\chi_{inelas} = Z \left[\ln \frac{a'^2 m_e^2 (1 + \ell)^2}{a'^2 t_{min} + 1} - 1 \right] ,$$

with

$$a = 184 (2.718)^{-1/2} \frac{Z^{-1/3}}{m_e} ,$$

$$a' = 1194 (2.718)^{-1/2} \frac{Z^{-2/3}}{m_e} .$$

The subscript $t = t_{min}$ in Eq. (1) means that when calculating the cross section for $\gamma + P_1 \rightarrow P_2 + k$, we assume not only the energy momentum conservation, $q + P_1 = P_2 + k$, but also $t = -q^2 = 0$ and the kinematics for $t = t_{min}$, namely,⁴ $P_{2\perp} = -k_{\perp}$ and $E_1 = E_2 + E_a$. Using these relations we obtain:

$$2P_1 \cdot k - m_a^2 = E_1^2 x \theta_a^2 + m_e^2 x + \frac{m_a^2 (1 - x)}{x} \equiv U , \quad (4)$$

$$2P_2 \cdot k + m_a^2 = \frac{U}{1 - x} , \quad (5)$$

$$2P_1 \cdot P_2 = \frac{Ux}{1 - x} + 2m_e^2 - m_a^2 . \quad (6)$$

The cross section for $\gamma + e \rightarrow e + a$ can be calculated using Feynman diagrams shown in Fig. 1(b):

$$\begin{aligned}
\frac{d\sigma(q + P_1 \rightarrow P_2 + k)}{d(P_1 \cdot k)} &= \frac{\alpha\alpha_a\pi}{(P_1 \cdot q)^2} \left[\frac{2(P_1 \cdot k)(P_2 \cdot k) - m_a^2(P_1 \cdot P_2) + 2m_e^2m_a^2}{(-m_a^2 + 2P_1 \cdot k)^2} \right. \\
&+ \frac{2(P_1 \cdot k)(P_2 \cdot k) - m_a^2(P_1 \cdot P_2) + 2m_e^2m_a^2}{(m_a^2 + 2P_2 \cdot k)^2} \\
&\left. - \frac{4(P_1 \cdot k)(P_2 \cdot k) + 2m_e^2m_a^2}{(-m_a^2 + 2P_1 \cdot k)(m_a^2 + 2P_2 \cdot k)} \right] ,
\end{aligned} \tag{7}$$

where $\alpha_a = g_a^2/4\pi$ with axion electron coupling $g_a a \bar{e} \gamma_5 e$.

Using Eqs. (4), (5) and (6), we obtain from Eqs. (1) and (7):

$$\begin{aligned}
\frac{d\sigma(P_1 + P_i \rightarrow P_2 + P_f + k)}{d\Omega_a dE_a} &= \frac{\alpha^2\alpha_a}{\pi} \frac{E_1}{U^2} \\
&\times \left\{ x^3 - \frac{2m_a^2x^2(1-x)}{U} + \frac{2m_a^2}{U^2} [m_a^2x(1-x)^2 + m_e^2x^3(1-x)] \right\} \chi .
\end{aligned} \tag{8}$$

After integrating with respect to angle, we obtain in the complete screening limit

($a^2t_{min} \ll 1$):

$$\begin{aligned}
\frac{d\sigma}{dx} &= 2r_0^2\alpha_a \frac{x(1 + \frac{2}{3}f)}{(1+f)^2} \left[Z^2 \ln(184 Z^{-1/3}) + Z \ln(1194 Z^{-2/3}) \right] \\
&+ 2r_0^2\alpha_a x \left[\frac{1}{3f^2} (1+f) \ln(1+f) - \frac{1+4f+2f^2}{3f(1+f)^2} \right] (Z^2 + Z) ,
\end{aligned} \tag{9}$$

where $f = (m_a^2/m_e^2)(1-x)/x^2$ and $r_0 = \alpha/m_e$.

If we set $m_a = 0$, Eq. (9) agrees with the result obtained by Donnelly *et al.*³

It is instructive to compare Eq. (9) with the corresponding formula for ordinary photon bremsstrahlung.⁵

$$\frac{d\sigma_b}{dx} = 4r_0^2 \alpha x^{-1} \left\{ \left(\frac{4}{3} - \frac{4}{3} x + x^2 \right) \times \left[Z^2 \ln(184 Z^{-1/3}) + Z^2 \ln(1194 Z^{-2/3}) \right] + \frac{1}{9} (1-x)(Z^2 + Z) \right\}. \quad (10)$$

The two equations have entirely different x dependence; the axion bremsstrahlung is highly peaked at $x = 1$, whereas the photon bremsstrahlung is infrared divergent at $x = 0$. In the photon bremsstrahlung, Eq. (10), the terms proportional to $(Z^2 + Z)$ are small compared with the logarithmic terms and thus they are often ignored, whereas in the axion bremsstrahlung, Eq. (9), the terms proportional to $(Z^2 + Z)$ are non-negligible especially near $x = 0$ where they even exceed the logarithmic terms. At $x = 1$ we have $f = 0$. Two terms inside the second square bracket of Eq. (9) have divergences, but they cancel one another resulting in a finite number. The ratio of the first term to the second term of Eq. (9) is $-R$ where

$$R \equiv \frac{(Z^2 + Z)}{2Z^2 \ln(184 Z^{-1/3}) + 2Z \ln(1194 Z^{-2/3})}, \quad (11)$$

which has a numerical value of $1/8.23$ for copper ($Z = 29$).

3. ELECTRON BEAM DUMP EXPERIMENT

In the beam dump experiment, the initial energy of the electron beam becomes degraded as it passes through a medium. An approximate formula for the energy distribution of the electron beam after passing through a medium of t radiation lengths can be written as⁶

$$I_e(E_0, E_1, t) = \frac{1}{E_0} \frac{[\ln(E_0/E_1)]^{bt-1}}{\Gamma(bt)} \quad (12)$$

$$\approx \frac{1}{E_0} \left(\frac{E_0 - E_1}{E_0} \right)^{bt-1} bt \quad , \quad (12')$$

where E_0 is the monochromatic electron energy at $t = 0$ and $b = 4/3$. In our calculation we use the simpler expression (12') instead of (12). This is justified because we are interested mostly in small values of $y = (E_0 - E_1)/E_0$ and thus $I_e(E_0, E_1, f)$ becomes very small as t gets large from the structure of (12') alone and the further suppression due to the Gamma function in the denominator of (12) at large t does not affect the numerical value of axion flux calculated. The number of axions produced per incident electron after going through a target of T radiation length is^{5,6}

$$\frac{dY}{dx} = \frac{NX_0}{A} \int_{E_a}^{E_0} dE_1 \int_0^T dt I_e(E_0, E_1, t) \frac{d\sigma}{dx'} \quad , \quad (13)$$

where $N = 6 \times 10^{23}$ is the Avogadro's number, X_0 is the unit radiation length^{5,7} of material in grams/cm², A is the atomic weight, T is the thickness of the target in units of radiation length, $x = E_a/E_0$ and $x' = E_a/E_1$.

Using Eq. (12'), the integration with respect to the target thickness can be carried out and we obtain:

$$\frac{dY_a}{dE_a} = \frac{\alpha_a}{2\alpha} \int_{E_a}^{E_0} dE_1 \frac{1 + y^{bT} (bT \ln y - 1)}{bE_0^2 y (\ln y)^2} \times x' \left\{ \frac{(1 + \frac{2}{3} f)}{(1 + f)^2} + 2R \left[\frac{1}{3f^2} (1 + f) \ln(1 + f) - \frac{1 + 4f + 2f^2}{3f(1 + f)^2} \right] \right\}, \quad (14)$$

where

$$y = \frac{E_0 - E_1}{E_0}, \quad x' = \frac{E_a}{E_1}, \quad f = \frac{m_a^2}{m_e^2} (1 - x') / x'^2,$$

and R is defined in Eq. (11). Eq. (14) shows that the yield becomes independent of Z of the target material if we ignore R . Also the yield becomes independent of thickness if T is more than a few radiation lengths, because $y^{bT} (bT \ln y - 1) \rightarrow 0$ for small y .

An axion decays into a pair of electrons with a lifetime of $\tau = [1/2 (\alpha_a m_a) (1 - 4m_e^2/m_a^2)^{1/2}]^{-1}$. At very relativistic energies, the energy distribution of e^+ or e^- from decay of an axion is flat, namely the number of electrons is proportional to dE_e/E_a with $0 < E_e < E_a$.

Let us consider an experimental setup as shown in Fig. 2. An electron with energy E_0 enters a target of length X_t (T radiation lengths) at $X = 0$. The electron loses energy very quickly within a few radiation lengths of the target and thus most of the axions, if they exist, as well as all other particles are created within the first few radiation lengths. The target length X_t must be long enough so that the electromagnetic shower is absorbed, and yet it should not be

too long in case the axion has a short lifetime. For example, a target consisting of 600 gm/cm^2 of uranium would have three times the nuclear interaction lengths,⁷ and one hundred times the unit radiation length⁷ and thickness of 31 cm. For an axion of mass 1.6 MeV and electron beam of 32 GeV, this setup will be sensitive to axions of lifetime longer than $\sim 10^{-14} - 10^{-13}$ sec depending upon the production cross section. Let us assume that a detector of e^+ and e^- is set up behind the target at $X = X_d$ as shown in Fig. 2. Only the electron pairs from axions which decay in the free space between X_t and X_d and those that decayed within the last couple of radiation lengths of the target can reach the detector. In order to simplify the calculation, we assume X_t and X_d to be much larger than unit radiation length of the target, so that all axions can be regarded as essentially produced at $X = 0$. The number of electrons or positrons in the energy interval dE_e at the detector due to decay of axions produced by each incident electron on the target can be obtained from

$$\left. \frac{dY_e}{dE_e} \right|_{X=X_d} = \left. \frac{dY_e}{dE_e} \right|_{X=X_t} + \int_{E_e}^{E_0} \frac{dE_a}{E_a} \left[\exp \left\{ -\frac{X_t}{\tau \gamma_a c} \right\} - \exp \left\{ -\frac{X_d}{\tau \gamma_a c} \right\} \right] \frac{dY_a}{dE_a}, \quad (15)$$

where the second term on the righthand side represents the electrons or positrons produced by the decay of axions in the open space between X_t and X_d . τ is the axion lifetime, $\gamma_a = E_a/m_a$ and dY_a/dE_a is given by Eq. (14) with $y^{bT} \rightarrow 0$ inside the integrand. The factor $1/E_a$ comes from the fact that the number of e^- or e^+ in dE_e is dE_e/E_a for each axion decay. The first term represents those electrons or positrons produced inside the target by decay of axions and can be written as

$$\left. \frac{dY_e}{dE_e} \right|_{X=X_t} = \int_0^{X_t} dX \int_{E_e}^{E_0} \frac{dE_a}{E_a} \int_{E_e}^{E_a} dE'_e \frac{dY_a}{dE_a} \frac{1}{\tau \gamma_a c} \exp \left\{ -\frac{X}{\tau \gamma_a c} \right\} I_e (E'_e, E_e, T - t) , \quad (16)$$

where $t = X\rho/X_0$ with ρ the density of the target and X_0 is the unit radiation length in gm/cm².

Since only the last few radiation lengths of the integration in Eq. (16) are significant, it should be much smaller than the other part of Eq. (15) if both $X_d - X_t$ and $\tau \gamma_a c$ are much bigger than the unit radiation length (in cm) of the target. Thus one can learn quickly whether the decay length of the axion is longer or shorter than a couple of radiation lengths by experimentally comparing the first and the second term in the right hand side of Eq. (15).

In our problem there are only two unknown parameters: α_a and m_a . Of course, the most important task is to show that the axion exists. The most convincing evidence would be to show that

1. e^+ and e^- at the detector have equal number and identical energy distribution;
2. the number of counts at $X = X_d$ is different from that at $X = X_t$ and the number varies with the distance ($X_d - X_t$) according to Eq. (15).

If it is shown that hardly anything is decaying between X_t and X_d , then it shows that either

- (1) the axion does not exist,
- (2) its production cross section is too small, or
- (3) its decay length, $\tau \gamma_a c$, is much smaller than the dump length.

Shorter dumps and higher energies (to increase γ_a in $\tau \gamma_a c$) can improve the

sensitivity of the experiment to short axion lifetimes. If an axion is shown to exist in the above manner, one can then compare the experimental yield and energy distribution with the theoretical result of Eq. (15) and thus obtain α_a and m_a .

4. DISCUSSIONS

4.1 X DEPENDENCE OF BREMSSTRAHLUNG OF PSEUDOSCALAR, SCALAR, VECTOR AND PSEUDOVECTOR PARTICLES

In order to understand qualitatively the behavior of the x dependence of the axion spectrum of Eq. (9), let us compare the relevant parts of the matrix element of the first diagram of Fig. 1(a) for emission of various particles:

Pseudoscalar:

$$\bar{U}(P_2) \gamma_5 \frac{1}{\not{P}_2 + \not{k} - m_e} \dots = \bar{U}(P_2) \gamma_5 \frac{\not{k}}{m_k^2 + 2P_2 \cdot k} \dots$$

Scalar:

$$\bar{U}(P_2) \frac{1}{\not{P}_2 + \not{k} - m_e} \dots = \bar{U}(P_2) \frac{\not{k} + 2m_e}{m_k^2 + 2P_2 \cdot k} \dots$$

Pseudovector:

$$\bar{U}(P_2) \gamma_5 \not{\epsilon} \frac{1}{\not{P}_2 + \not{k} - m_e} \dots = \bar{U}(P_2) \gamma_5 \frac{2P_2 \cdot \epsilon + \not{\epsilon} \not{k} + 2m_e \not{\epsilon}}{m_k^2 + 2P_2 \cdot k} \dots$$

Vector:

$$\bar{U}(P_2) \not{\epsilon} \frac{1}{\not{P}_2 + \not{k} - m_e} \dots = \bar{U}(P_2) \frac{2P_2 \cdot \epsilon + \not{\epsilon} \not{k}}{m_k^2 + 2P_2 \cdot k} \dots$$

The cross sections are obtained by squaring the matrix elements, averaging over the spins and multiplying the results by the phase space $\int d^2k/(2E_k)$. The γ_5 's in the righthand side of the above equations anticommute through the γ matrices and annihilate each other in the trace, so they do not change the behavior of the cross section in the high energy limit where the mass of the electron becomes negligible compared with its energy. Thus we observe that in the high energy limit, the emissions of scalar and pseudoscalar particles have similar x dependence and similarly those for vector and pseudovector particles. We also notice that as $k \rightarrow 0$, the matrix element vanishes for emission of pseudoscalar particles. This explains the drastically different x dependence between Eqs. (9) and (10). In the limit that electron has zero mass, its helicity is changed when either a scalar or a pseudoscalar particle is emitted, whereas the helicity is conserved when either a vector or a pseudovector particle is emitted. Thus the difference in the x dependence in Eqs. (9) and (10) is related to the helicity flip in the former and the helicity conservation in the latter. In order to see this, we multiply γ_5 from the right of each of the four equations given above and move it through until it reaches to the right of $\bar{U}(P_2)$. We notice that the sign of γ_5 is changed for scalar and pseudoscalar, but it is unchanged for vector and pseudovector if we set $m_e = 0$ for all cases. We further observe that \not{k} in the numerator is needed to change the sign of γ_5 for scalar and pseudoscalar cases and this is the reason for the absence of infrared divergence and the peaking of the cross section near $x = 1$ for these two cases.

4.2 AXION PRODUCTION IN PROTON BEAM DUMP

In proton machines axions can in principle be created by protons, pions, muons, photons and e^\pm 's in the dump. The e^\pm 's are produced by the photons from π^0 decay. Our cross section can of course be used to calculate axion flux from these e^\pm 's. In the electron beam dump, axions are created mostly in the first couple of radiation lengths, whereas in the proton machine, pions are created throughout several interaction lengths, which is much longer; for example⁷ one interaction length equals 94 and 622 radiation lengths, respectively, for copper and uranium.

We show in the following that even in the proton dump, most of the axions are likely created by the axion bremsstrahlung from the e^\pm in the dump.

Bremsstrahlung of axions by hadrons

Bremsstrahlung of axions by hadrons can be estimated in the following way. In Fig. 1(a) the electron is replaced by a hadron and the photon is replaced by a gluon or a pomeron. g_a for coupling between electron and axion is proportional to m_e but for hadrons it is proportional to the quark masses. Weinberg suggests⁸: $m_u = 4.2$ MeV, $m_d = 7.5$ MeV. The hadronic cross section from nuclear target is proportional to $A^{2/3}$ in contrast to $Z^2 \ln(184 Z^{-1/3})$ in Eq. (9). The factor $\alpha_0^2 = \alpha^2/m_e^2$ in Eq. (9) must also be replaced by $\sim 1/M_h^2$ because the strength of hadronic interaction is of order one and the bremsstrahlung emission is proportional to inverse mass squared of the hadron.

The qualitative argument given above leads to the following approximate relation:

$$\begin{aligned}
& \frac{\sigma(\text{pion} + A \rightarrow \text{axion} + \text{anything})}{\sigma(e + A \rightarrow \text{axion} + \text{anything})} \\
& \approx \left(\frac{m_q}{m_e}\right)^2 \frac{\sigma(\gamma + A \rightarrow \text{hadronic final state})}{\sigma(\gamma + A \rightarrow e^+e^- + \text{anything})} \quad (17) \\
& = \left(\frac{m_q}{m_e}\right)^2 \frac{100 \mu b A^{2/3}}{\frac{14}{9} \alpha r_0^2 \chi(\ell = 0)} \\
& = \left(\frac{m_q}{m_e}\right)^2 \frac{1}{3900} \text{ for copper target .}
\end{aligned}$$

This ratio is very critically dependent upon the quark mass m_q and A . Using $m_d = 7.5$ MeV for m_q the ratio given by Eq. (17) is much less than unity for a copper target. For axion bremsstrahlung from a proton, a factor of $(m_\pi/m_P)^2 \equiv 0.02$ must be multiplied on the right hand side of Eq. (17).

In the proton dump the numbers of π^+ , π^- and π^0 are roughly equal. Each π^0 produces 2γ and each γ produces a pair of e^+e^- with almost 100% efficiency in a thick target. Thus axion bremsstrahlung from hadrons is likely not important compared with that from e^\pm in the dump.

Axion production by muons

Very few pions decay into μ 's at high energies. Also axion bremsstrahlung from muons has almost the same cross section as that from electrons because the increase in the coupling constant of axion to muon is exactly cancelled out by the kinematical factor of m_μ^2 in the denominator due to the fact that it is harder

to bremsstrahlung from heavier particles. Therefore axion bremsstrahlung from muon is negligible compared with that from the e^\pm in the proton beam dump.

Axion production by photons

Axions can be created by photons through the Primakoff effect $\gamma + Z \rightarrow$ axion $+ Z$ or lepton pair production $+$ axion as shown in Fig. 3(a) and 3(b), respectively. The angular distribution of axions from the Primakoff⁹ mechanism can be obtained from Fig. 3(a):

$$\frac{d\sigma}{d\Omega_a} (\gamma + Z \rightarrow a + Z) = \frac{8\Gamma(a \rightarrow \gamma\gamma)}{m_a^3} \alpha Z^2 F^2 \frac{P^4 \sin^2 \theta}{t^2} , \quad (18)$$

where $\Gamma(a \rightarrow \gamma\gamma)$ is the partial decay width of axion into 2γ and is given approximately² by $\Gamma = \alpha^3 m_a^3 / M_W^2$, P is the momentum of the axion, $Z^2 F^2$ is the target form factor. In our case the $t_{min} = (m_a^2 / 2k)^2$ is so small that the atomic form factors⁵ must be used when t is small ($t \leq 7.39 m_e^2$) and a nuclear form factor^{4,5} must be used for large t ($t > 7.39 m_e^2$). Integrating (18) with respect to the solid angle using atomic and nuclear form factors given in Refs. 4 and 5, we obtain

$$\begin{aligned} \sigma(\gamma + Z \rightarrow a + Z) &= \frac{16\pi\Gamma(a \rightarrow 2\gamma)}{m_a^3} \\ &\times \alpha \left\{ Z^2 \ln(184 Z^{-1/3}) + Z \ln(1194 Z^{-2/3}) + Z^2 \left[\ln \left(\frac{\sqrt{d}}{m_e} \right) - 2 \right] \right\} \\ &= O \left(\frac{\alpha^4}{M_W^2} \right) Z^2 , \end{aligned} \quad (19)$$

where $\sqrt{d} = \sqrt{6} / (1.2 \times A^{1/3} \text{ fermi}) = 403 A^{-1/3} \text{ MeV}$. In Eq. (9) α_a is $O(e^2 m_e^2 / M_W^2)$.

Hence comparing Eq. (19) with Eq. (9) we conclude¹¹

$$\frac{\sigma(\gamma + Z \rightarrow a + Z)}{\sigma(e + Z \rightarrow e + a + Z)} \equiv \alpha \quad , \quad (20)$$

and thus the Primakoff mechanism of producing an axion is negligible compared with the axion bremsstrahlung by electron.

The axion production from $\gamma + Z \rightarrow e^+e^-aZ$ as shown in Fig. 3(b) is also negligible compared with axions from the process $e + Z \rightarrow e + a + Z$. Fig. 3(b) says that for each e^+ or e^- produced by pair production, there will be roughly α_a axions produced through the mechanism of Fig. 3(b). But Eq. (14) says that for each e^+ or e^- produced, the number of axions produced by the process $e + Z \rightarrow e + a + Z$ is roughly α_a/α .

4.3 TARGET FORM FACTORS

Our Eq. (8) is applicable for any degree of atomic screening whereas Eq. (9) is true only for complete screening, *i.e.*, $a^2t_{min} \ll 1$. The other limiting case $a^2t_{min} \gg 1$ is called no screening, which happens when the axion is heavier and the incident electron energy is lower. In the no screening case, the dependence on atomic radius drops out from expressions for χ_{elas} and χ_{inelas} . After angular integration of Eq. (8) we obtain for the no-screening limit:

$$\frac{d\sigma}{dx} (e + Z \rightarrow e + a + Z) = 2r_0^2 \alpha_a \frac{x(1 + \frac{2}{3}f)}{(1+f)^2} Z^2 \left\{ \ln \left[\frac{2E_1(1-x)}{m_e x(1+f)} \right] - \frac{1}{2} \right\} \quad , \quad (21)$$

where all the notations are the same as those that appeared in Eq. (9). The term proportional to Z is left out because when t_{min} becomes large the atomic electrons cease to be an efficient target for production. When t_{min} becomes even larger, say tens of MeV, the nuclear form factors become important. In all cases,

only the expression for χ in Eq. (8) becomes different. The necessary expressions for χ for all target materials and all conceivable t_{min} are treated in Refs. 4 and 5. Equation (21) was first obtained by Zhitnitskii and Skovpen¹⁰ without using the Weizsacker–Williams method. As mentioned earlier, in most of the experiments we have in mind $E_1 = 1 \sim 100$ GeV and $m_a \sim 1.7$ MeV, the atomic screening is important and hence Eq. (9) should be used instead of Eq. (21). The atomic parameters a and a' given in the definition of χ , Eq. (11), are suitable only for atomic elements with $Z \geq 5$. For atomic elements with smaller Z the parameters given in Table B.4 of reference 5 should be used.

4.4 WEIZSACKER–WILLIAMS APPROXIMATION

This paper is another demonstration of how the generalized Weizsacker–Williams method developed in Ref. 4 can be used in deriving simple formulas for a complicated problem. With this method formula such as Eq. (8) can be derived in a matter of one afternoon whereas it might take a couple of months of hard work to derive it using a more conventional method.

Acknowledgments

The author wishes to thank James D. Bjorken, Michael Riordan and Charles Brown for discussions and useful criticism of the manuscript.

REFERENCES

1. T. Cowan *et al.*, *Phys. Rev. Lett.* **54** , 1761 (1985) .
2. R. Peccei and H. Quinn, *Phys. Rev. Lett.* **38** , 1440 (1977); S. Weinberg, *Phys. Rev. Lett.* **40** , 223 (1978); F. Wilczek, *Phys. Rev. Lett.* **40** , 279 (1978).
3. T. W. Donnelly *et al.*, *Phys. Rev. D***18** , 1607 (1978).
4. K. J. Kim and Y. S. Tsai, *Phys. Rev. D***8** , 3109 (1973).
5. Y. S. Tsai, *Rev. Mod. Phys.* **46**, 815 (1974).
6. Y. S. Tsai and Van Whitis, *Phys. Rev.* **149** , 1248 (1966).
7. Particle Data Group, *Rev. Mod. Phys.* **56**, S53 (1984).
8. S. Weinberg, in *A Festschrift for I. I. Rabi*, ed. L. Motz (New York Academy of Sciences, New York, 1977).
9. H. Primakoff, *Phys. Rev.* **81** , 899 (1951).
10. A. R. Zhitnitskii and Yu. I. Skovpen, *Yad. Fiz.* **29**, 995 (1979), trans. *Sov. J. Nucl. Phys.* **29** (4), 513 (1979).

FIGURE CAPTIONS

Figure 1. (a) Axion bremsstrahlung by an electron in the atomic target

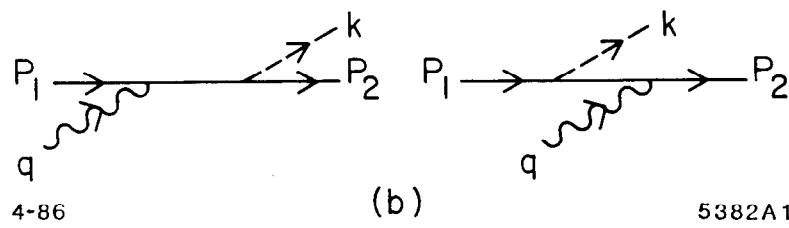
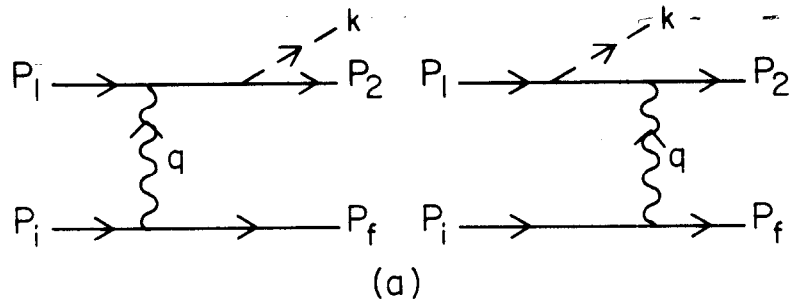
$$e + P_i \rightarrow e + P_f + \text{axion};$$

(b) axion production by $e\gamma$ collision: $\gamma + e \rightarrow \text{axion} + e$.

Figure 2. Experimental arrangement for axion production and detection.

Figure 3. (a) Production of axion by Primakoff effect.

(b) axion bremsstrahlung by lepton pair.



4-86

5382A1

Fig. 1

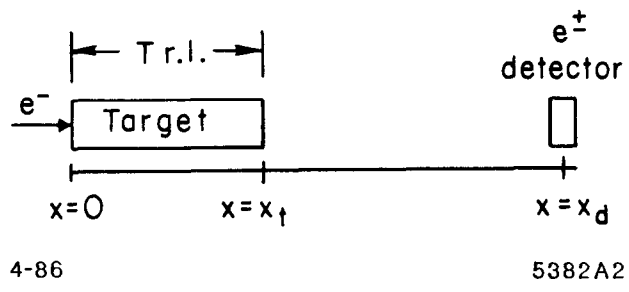


Fig. 2

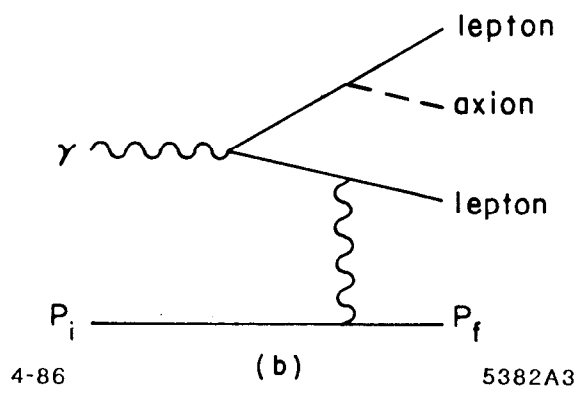
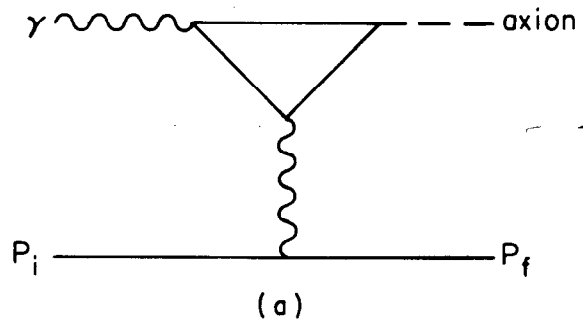


Fig. 3